Dynamic Heterogeneity in Miscible Polymer Blends with Stiffness Disparity: Computer Simulations Using the Bond Fluctuation Model

Sudesh Kamath,† Ralph H. Colby,* and Sanat K. Kumar‡

Department of Materials Science and Engineering, Pennsylvania State University, University Park, Pennsylvania 16802

Received May 22, 2003; Revised Manuscript Received August 18, 2003

ABSTRACT: The dynamics of athermal polymer blends with stiffness disparities are studied using computer simulations of the bond-fluctuation model. For mixtures of ten-mer chains, we see a difference in the temperature dependence of the diffusion coefficients of the two blend components for all blend compositions with appreciable amounts of the more flexible component. Hence, our model system can qualitatively capture the composition dependence of dynamic heterogeneity that is observed experimentally in miscible polymer blends. While blends of ten-mer chains display clear evidence for dynamic heterogeneity, the dynamics of the two components in blends of dimers are identical over the entire temperature range studied. Shorter chain systems experience smaller concentration fluctuations and smaller contributions from chain connectivity, suggesting that local concentration variations play a critical role in the dynamic heterogeneity that is observed experimentally in miscible polymer blends with weak interactions. The diffusion coefficient of dilute flexible chains in a matrix of stiff chains is identical to the diffusion coefficient of the matrix chains at all temperatures, clearly demonstrating that inherent mobility differences of the two chains cannot solely explain blend dynamics.

I. Introduction

The blending of two miscible polymers is a cost-effective method for producing new materials with tailored properties. Although thermodynamically miscible, and hence molecularly mixed, often the dynamics of the two components in the blend exhibit different temperature dependences (dynamic heterogeneity). This heterogeneity causes a breakdown in the empirical time−temperature superposition principle. Such thermorheological complexity has been reported for miscible blends with weak interactions, where the two components have very different glass transition temperatures (T_g).[1−8] At any given temperature, the relaxation of the high-T_g component in the blend is faster compared to its pure component value, while that of the low-T_g component is slowed down on blending. While some workers attribute this phenomenon to concentration fluctuations[7−10] and chain connectivity effects,[7,8,11] others have argued that thermorheological complexity only reflects inherent differences in the local dynamics of the constituents.[12] Moreover, there are no data that clearly delineate the molecular origins of dynamic heterogeneity. Since computer simulations probe the system at a molecular level, simulations are an ideal tool to study the effects of various system parameters on dynamic heterogeneity as well as to gain insights into its molecular origins.

Most miscible polymer blends exhibit dynamic heterogeneity at temperatures close to the blend T_g, where segmental relaxation times are $\sim 10^{-6}-10^{0}$ s. Since the longest molecular dynamic simulations can only probe time scales on the order of microseconds, we have employed dynamic Monte Carlo simulations to probe longer time scales. In this context we stress that the mapping of Monte Carlo time into experimental times remains an open question. Further, since Monte Carlo simulations do not keep track of the momenta of the particles, it follows that these simulations ignore any hydrodynamic interactions. With these caveats, however, we note that previous Monte Carlo simulations of the bond fluctuation model have properly captured the crossover of chain dynamics from the Rouse model to reptation with increasing chain length, giving us considerable confidence in the results obtained. Experimental results on several miscible polymer blends[1−8] have established that dynamic heterogeneity results when (a) the two blend components have weak interactions and (b) there is sufficient disparity in the two component glass transition temperatures, regardless of the molecular details of the component polymers. These findings suggest that a coarse grained model is sufficient if the purpose is to establish the origins of dynamic heterogeneity in miscible polymer blends.

In this paper, we use Monte Carlo simulations to study the dynamics of a miscible bond fluctuation polymer blend where the two components have a stiffness disparity.[13,14] This model has been used extensively to study blend thermodynamics.[15,16] First, we show that this coarse-grained model can qualitatively capture all of the experimentally observed features of dynamic heterogeneity. Then system parameters are varied to study the effects of concentration variations and differences in inherent mobilities of the constituents on the dynamics of the two blend components.

II. Model and Simulation Details

In the bond fluctuation model,[13] each monomer occupies eight adjacent sites on a simple cubic lattice. Monomers are connected by bonds whose lengths, b, vary in the range $2 \le b \le \sqrt{10}$. To avoid bond crossing, only six possible bond classes are allowed: [2,0,0], [2,1,0], [2,1,1], [2,2,1], [3,0,0], [3,1,0], where all permutations of positive or negative values of bond vectors are

† Present address: Department of Chemistry, University of Tennessee, Knoxville, TN 37996.
‡ Present address: Department of Chemical Engineering, Rensselaer Polytechnic Institute, Troy, NY 12180.
* To whom correspondence should be addressed.

10.1021/ma034682x CCC: $25.00
Published on Web 09/30/2003

utilized. This leads to 108 possible bond vectors. Thus, the model has some of the flexibility associated with an off-lattice model while maintaining the advantages of working on a lattice. Double occupancy of a lattice site is prohibited, and energetics are introduced by a two-level Hamiltonian which favors longer bonds at lower temperatures.

$$H = \begin{cases} 0 & \text{if } b \in [3,0,0] \\ \epsilon & \text{otherwise} \end{cases} \quad (1)$$

Temperature is defined in reduced units: $T^* \equiv k_B T/\epsilon$, where k_B is Boltzmann's constant. Previous studies have demonstrated that this model can qualitatively capture the vitrification of polymers.[17,18]

Experiments on miscible blends[1−8] suggest that dynamic heterogeneity is observed when the two blend components have weak interactions *and* there is a disparity in their inherent dynamics, reflected in differences in their glass transition temperatures T_g or Vogel temperatures, T_0. The parameter ϵ directly determines the mobility of a polymer and hence its Vogel temperature, T_0. In this study, we have set $\epsilon_A = 1$ and $\epsilon_B = 2$, where A and B are the low-T_g and high-T_g components in the blend, respectively. Since the energetics of the system in our Monte Carlo simulations are controlled by the parameter ϵ, chains of type B have twice the energetic barrier to motion as chains of type A. This indicates that the Vogel temperature for a melt of B chains should be twice that of a melt of A chains, and our data on pure melts of A and B chains corroborate this fact.[14] There are no other interactions in the system.

Thus, our system satisfies all the conditions that are common for miscible blends exhibiting dynamic heterogeneity, namely, weak interactions between the two blend components and a substantial difference in the Vogel temperatures of the two blend components. We have considered two different chain length blends in our study. The majority of our calculations were for blends of ten-mers (chains with $N = 10$ monomers), and a few were for blends of dimers ($N = 2$). For all $N = 10$ chain simulations, we employ a 60^3 cubic lattice with periodic boundary conditions. Since the Hamiltonian (eq 1) favors bonds in the [3,0,0] bond class at lower temperatures, a chain of length $N = 10$ will effectively "block" 116 lattice sites. Eighty of these sites are occupied by the monomers, and an additional 36 account for lattice sites blocked by the presence of the [3,0,0] bonds. Thus, the system gets spatially frustrated at monomer densities greater than $\rho = 0.7$. For all higher densities, it is not possible for all bonds to simultaneously reach their ground state. With this criterion in mind, we simulated a monomer density of $\rho = 0.8$ (2160 chains). For the dimer simulations ($N = 2$) the system gets spatially frustrated at monomer densities greater than $\rho = 0.8$, and hence we studied a monomer density of $\rho = 0.9$ to impose a similar degree of spatial frustration as the $N = 10$ system. The dimer systems used 3600 dimers on a 40^3 lattice.

Starting configurations were obtained by filling the simulation box with chains having all bonds in the [2,0,0] bond class. Chains were then randomly removed until the desired monomer density was reached. Next, chains were randomly tagged as type B until the desired composition was achieved. The system was then equilibrated at infinite temperature. For the $N = 10$ system, we have simulated blends having $\phi_B = 0.25$, $\phi_B = 0.5$, and $\phi_B = 0.75$, while for the $N = 2$ system, we have only studied a $\phi_B = 0.5$ mixture, where ϕ_B is the volume fraction of the high-T_g B chains in the system. Starting configurations for lower temperatures were equilibrated configurations obtained at the next highest temperature.

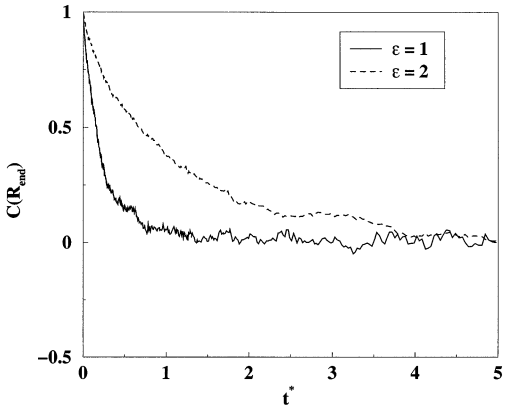

Figure 1. Time dependence of the autocorrelation function for the end-to-end vector for both components in a $\phi_B = 0.75$ blend at a temperature $T^* = 0.55$. $C(R_{end})$ is the end-to-end vector autocorrelation function, and t^* represents time in units of 10^6 Monte Carlo steps.

The system was simulated using the standard Metropolis Monte Carlo technique. Two types of moves were employed during equilibration: reptation and single monomer flips. In a reptation move[19] a monomer is transferred from one end of the chain to the other. A single monomer move corresponds to moving a randomly chosen monomer by one lattice site in one of the six lattice directions. An important consideration for our studies is equilibrium. As the temperature is decreased, single monomer moves involve moving a bond from its ground state to a higher energy state, which is a low probability event. In addition, the new site needs to be empty. In conjunction, these factors make it difficult to equilibrate the system using single monomer moves. The reptation algorithm, on the other hand, only involves removing a bond from one end of the chain and regrowing it at the other end. If the regrown bond is in the ground state, then the only constraint for motion is the availability of free lattice sites. Therefore, the system was equilibrated using the reptation algorithm while dynamics were studied using purely single monomer moves, as suggested by Binder.[19] Time in the dynamics simulations is defined in Monte Carlo steps (MCS). Each Monte Carlo time step corresponds to an average of one attempted move per monomer. To check for equilibrium, we have monitored three quantities: (a) The autocorrelation function of the end-to-end vector, $C(R_{end})$, defined as $C(R_{end}) = \langle R(t)\cdot R(0)\rangle/\langle R(0)^2\rangle$, where $R(t)$ and $R(0)$ are the end-to-end vectors at times t and 0, respectively. $C(R_{end})$ goes to zero in the long time limit. (b) The mean-square displacement of the center of mass, which becomes diffusive at long times. (c) The self-intermediate structure factor, which goes to zero in the long time limit. The system is considered to be equilibrated only if *all three criteria are simultaneously satisfied for both components*. Figure 1 shows a plot of the correlation function of the end-to-end vector, $C(R_{end})$, for both components in a $\phi_B = 0.75$ blend at a temperature $T^* = 0.55$. It is clear that the $C(R_{end})$ values for both components have reached a value of zero by the

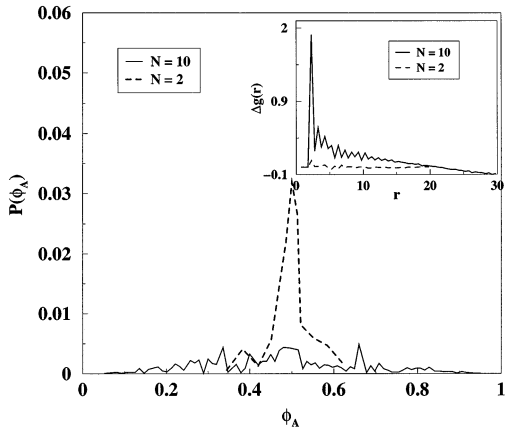

Figure 2. Probability $P(\phi_A)$ of finding a 10^3 subvolume with composition ϕ_A for a $\phi_B = 0.5$ blend of $N = 10$ chains (solid curve) as well as $N = 2$ dimers (dashed curve) at $T^* = 0.5$. The inset shows a plot of the intermolecular $\Delta g(r)$ defined by eq 3 for the $N = 10$ blend and the $N = 2$ dimers with $\phi_B = 0.5$ at $T^* = 0.5$.

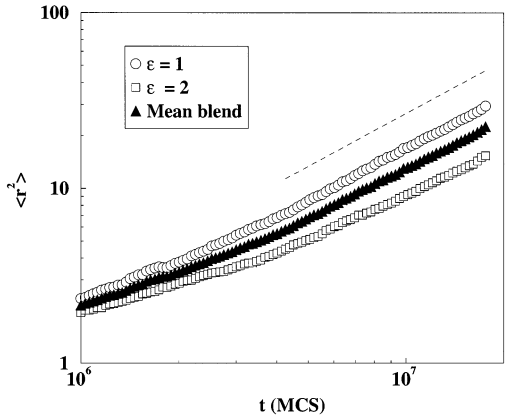

Figure 3. Mean-square center of mass displacement, $\langle r^2 \rangle$, as a function of time, t, in Monte Carlo steps (MCS) for each component in a $\phi_B = 0.5$ blend of $N = 10$ chains at a temperature $T^* = 0.45$. The mean blend data (filled triangles) correspond to $\langle r^2 \rangle$ for all monomers in the blend if we do not distinguish between the two blend components. The dashed line has a slope of unity.

end of the run. However, the stiffer chains take ~4 times longer to reach a $C(R_{end}) = 0$ than the flexible chains, a fact that is also reflected in its smaller diffusion coefficient as we shall discuss below.

After equilibration, we first quantify the spontaneous (thermally driven) concentration fluctuations in our blends, which are expected by some models to be critically important in determining blend dynamics.[9,10,20] Thermodynamics relate the mean-square concentration fluctuation to the zero wavevector limit of the scattering function ($\langle(\Delta\phi)^2\rangle \sim S(0)$).[21] The random phase approximation[21,22] leads to

$$\frac{1}{S(0)} = \frac{1}{\phi_A N_A} + \frac{1}{\phi_B N_B} - 2\chi \qquad (2)$$

where N_A and N_B are the numbers of monomers in the low-T_g and high-T_g component polymers and χ is the Flory interaction parameter describing the net energetic interaction between dissimilar component monomers. For a $\phi_A = \phi_B = 0.5$ blend with $\chi = 0$ and $N_A = N_B = 2$, the random phase approximation yields $S(0) = 0.5$, while for $N_A = N_B = 10$, $S(0) = 2.5$. Since the theory[9,10,20] predicts that suppressing concentration fluctuations diminishes dynamic heterogeneities in the blend, we expect that the $N = 2$ blend will be less heterogeneous than the longer chain blend. To test this hypothesis, we have simulated a blend of dimers ($N = 2$) with $\phi_B = 0.5$ having the same stiffness disparity as the $N = 10$ blend.

To quantify concentration variations, we have calculated two quantities. First, we divide the system into subvolumes of size 10^3 and measure the concentration of A and B monomers in each subvolume. We can thus generate a concentration distribution which is a direct measure of concentration fluctuations in the system. Figure 2 shows that the distribution of concentrations is much sharper for the dimer blend. We also calculate

$$\Delta g(r) = g_{AA}(r) + g_{BB}(r) - 2g_{AB}(r) \qquad (3)$$

where $g_{xy}(r)$ is the *intermolecular* pair distribution function for monomers of type x and y. $\Delta g(r)$ would identically equal 0 for all r in systems where both components are uniformly mixed, and hence any deviations from 0 are a measure of nonuniform packing ("concentration fluctuations"). The lower the value of $\Delta g(r)$, the smaller the concentration fluctuations at the length scale r. The inset in Figure 2 compares $\Delta g(r)$ for $N = 10$ blends and $N = 2$ blends at $\phi_B = 0.5$ and $T^* = 0.5$. Note that for this calculation we have intentionally excluded the intramolecular contributions to the radial distribution functions for AA and BB to eliminate connectivity effects. From the inset, we see that concentration fluctuations are suppressed in the dimer blend, as expected by thermodynamics (eq 2).

III. Dynamics

To study dynamics, we simulate motion in blends at various temperatures using purely single monomer moves. The time dependence of the mean-square displacement of the center of mass of the chains for each component in a $\phi_B = 0.5$ blend of $N = 10$ chains at $T^* = 0.45$ is shown in Figure 3. The "mean blend" data correspond to an average over all chains in the system without distinguishing between the two components. The flexible component ($\epsilon = 1$) moves faster than the mean, while the stiff component ($\epsilon = 2$) moves slower than the mean. At long times, the mean-square displacement of the center of mass is proportional to time, allowing for the calculation of the diffusion coefficient: $D = \lim_{t\to\infty} \langle r^2 \rangle / 6t$. Parts a and b of Figure 4 show plots of the temperature dependence of diffusion coefficients for each component in the blend, as well as the pure component melts, for the $N = 2$ and $N = 10$ systems, respectively. The dynamics of both components in the $N = 2$ blend are virtually identical, whereas those in the $N = 10$ blend are noticeably different. Thus, suppressing concentration fluctuations leads to a decrease in dynamic heterogeneity, as predicted by the theory.[9,10,20] However, it is important to point out that models for blend dynamics that rely on chain connectivity effects and explicitly ignore concentration fluctuations also expect a qualitatively similar trend.[7,8,11]

In the limit $T^* \to \infty$, all diffusion coefficients are identical since stiffness, which is the only parameter that distinguishes the two components, is irrelevant. At lower temperatures, the two components in the $N = 10$ blend have different temperature dependences of their diffusion coefficients. The stiffer component is faster in the blend while the flexible component is slowed down relative to its single component melt value, in agree-

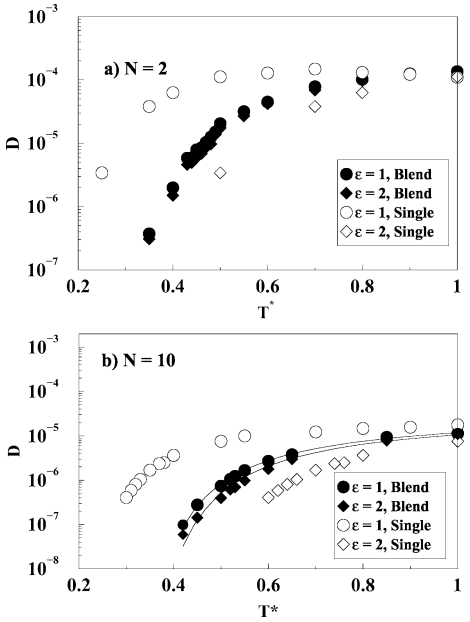

Figure 4. Diffusion coefficients of the pure components (open symbols) and each component in a $\phi_B = 0.5$ blend (filled symbols). (a) $N = 2$, (b) $N = 10$.

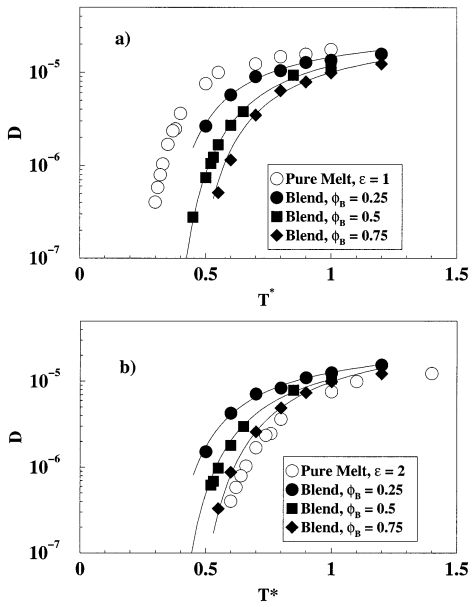

Figure 5. Diffusion coefficients for (a) the flexible component and (b) the stiff component in various blends of $N = 10$ chains as a function of temperature. The diffusion coefficients for the corresponding pure melts are also shown as open symbols for reference.

ment with experimental findings. Note that, unlike the experimental data on miscible blends, where the difference in the relaxation times of the two components can be an order of magnitude, the difference in the D values of the two components in our system is smaller than a factor of 2. Presumably, this is a direct consequence of the short chains used in our simulations. However, our simulations can qualitatively reproduce the dynamic heterogeneity observed experimentally in miscible polymer blends, and it is clear that the two components should have different extrapolated Vogel temperatures, T_0.

To quantify this statement, we have fit the diffusion coefficients of both components to a Vogel equation

$$D \propto \exp\left(\frac{-BT_0}{T - T_0}\right) \tag{4}$$

Figure 4b shows representative fits for the $\phi_B = 0.5$ blend of $N = 10$ chains. We find that $T_0^A = 0.285$ and $T_0^B = 0.295$, quantifying the dynamic heterogeneity in this blend. The corresponding values for single component A and B melts are $T_0^A = 0.22$ and $T_0^B = 0.44$, respectively. The Vogel temperature for the blend, T_0^{Fox}, is 0.293 as predicted by the Fox equation, $1/T_0^{Fox} = \phi_A/T_0^A + \phi_B/T_0^B$. Hence, we see that the stiff blend component has a Vogel temperature slightly larger than what is expected by the Fox equation, while the flexible blend component has a Vogel temperature that is smaller than the Fox equation prediction.

To study the effect of composition on component dynamics in the blend, we have carried out similar studies on blends containing $\phi_B = 0.0046$, $\phi_B = 0.25$, $\phi_B = 0.75$, and $\phi_B = 0.9954$. Parts a and b of Figure 5 show plots of the diffusion coefficients of the flexible and stiff components in the blend, respectively, for $\phi_B = 0.25$, 0.5, and 0.75. The corresponding values for each single component melt are shown for reference. From Figure 5, we see that the dynamics of the flexible component get progressively slower as the fraction of stiff component is increased, while the dynamics of the stiff component get progressively closer to those of a pure melt of stiff chains. We have also calculated the Vogel temperature T_0 for both blend components for all compositions by fitting to eq 4. Figure 6 shows a plot of the Vogel temperatures in the blends as a function of the composition of the stiff component, ϕ_B. The line represents the Fox equation prediction for the blend. The differences in T_0 of the components in our simulated blend are quite similar to experimental results based on the temperature dependence of the average segmental relaxation time for $\phi_B = 0.25$, 0.5, and 0.75 PI/PVE blends.[23] For these compositions, the high-T_g (stiff) component has T_0 slightly above the Fox equation prediction, while the low-T_g (flexible) component has a lower T_0. The exception (at $\phi_B = 0.0046$) will be discussed in the next section. In particular, the experimental result[23] that the largest differences in component Vogel temperatures are seen for blends rich in the low-T_g component is also seen in our simulations.

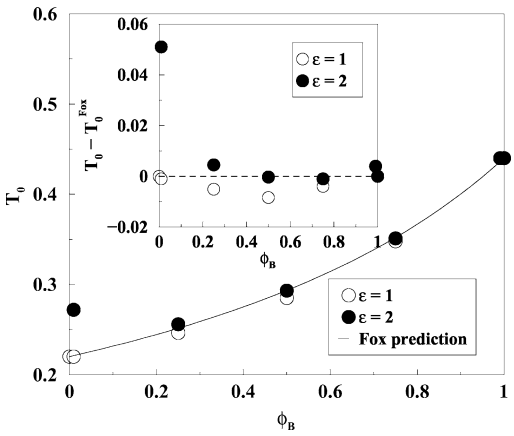

Figure 6. Vogel temperature, T_0, evaluated from the temperature dependence of diffusion coefficients for both blend components as a function of the volume fraction of the stiff component, ϕ_B. The solid line represents the Fox prediction for the Vogel temperature for the blend.

The ten-mer chains we have studied are sufficiently short that they can be completely in regions of fast or slow dynamics (see Figure 2). In this sense, then, the dynamics of these short chains directly reflect segmental dynamics. It is very important to point out that real (much longer) polymer chains will sample a broad range of environments and will always have some of their monomers in the slowest possible environments. Hence, in this limit the chains can have very different temperature dependences for average segmental dynamics and terminal dynamics. For long polymers, terminal dynamics (reflected in the diffusion coefficient) appears to be governed by the slowest segmental dynamics of the monomers on that chain. This can make the Vogel temperature of the high-T_g component much larger than that predicted by the Fox equation, as seen by Kim et al.[24] in a 50/50 blend of polystyrene and tetramethylpolycarbonate, for example.

The asymmetry observed in Figure 6 is exactly what is predicted by recent models for the average segmental dynamics of miscible polymer blends. A combination of two effects create this asymmetry: concentration fluctuations[9,10,20,25] and chain connectivity.[11,25] Concentration fluctuations are sufficiently strong in weakly interacting polymer blends that local compositions vary over the entire possible range of compositions ($0 < \phi_B < 1$). However, two compositions dominate segmental dynamics. One is the most probable local composition, which is the mean composition of the blend augmented by chain connectivity effects, see below. The other important composition is the one corresponding to the fastest possible environment: local regions of nearly pure low-T_g component. While the mean blend composition is a likely composition for the regions surrounding either low-T_g or high-T_g monomers, the local regions of nearly pure low-T_g component can only surround monomers of the low-T_g component. Hence, it is the low-T_g component that diffuses faster than what is expected by the Fox equation, while the high-T_g component roughly obeys the Fox equation prediction. In blends with very different component glass transitions, this asymmetry even makes the segmental relaxation time distribution of the low-T_g component bimodal.[10,20] This has been observed in dielectric measurements on blends of poly(vinyl methyl ether) (PVME) and polystyrene.[26] PVME has a bimodal distribution of segmental relaxation times, with one peak corresponding to the mean blend composition and the other corresponding to regions of nearly pure PVME (the low-T_g component).

However, as Figure 2 clearly shows, concentration fluctuations are suppressed as the chain length of the blend components is shortened. For this reason, while the concentration fluctuations of our ten-mer chains are larger than for dimers, they are not nearly as large as those in real polymer blends. The effect of chain connectivity plays an important role in the asymmetry seen in Figure 6. The connected nature of polymer chains makes the average local composition surrounding an A monomer richer in component A than the average local composition surrounding a B monomer.[7,8,11,25] Just as in real polymer blends, the relative magnitudes of the effects of concentration fluctuations and chain connectivity are difficult to assess because we do not know a priori what size scale is relevant for cooperative motion.

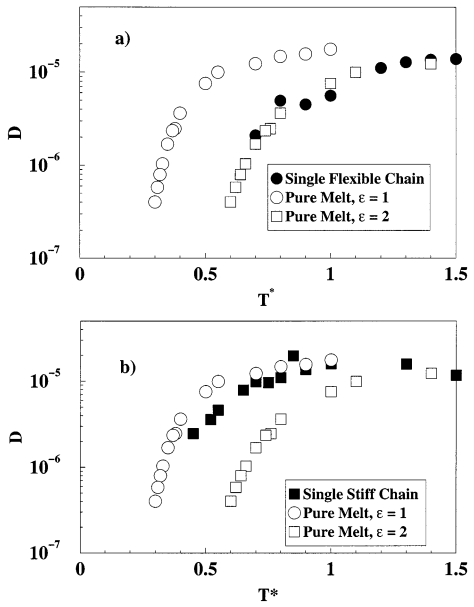

Figure 7. Temperature dependence of diffusion coefficients for (a) a single flexible chain in a matrix of stiff chains and (b) a single stiff chain in a matrix of flexible chains. The diffusion coefficients for pure melts of flexible chains and pure melts of stiff chains are shown as open symbols for comparison.

IV. Dilute Blends

Recent arguments[12] have suggested that component dynamics in a polymer blend are controlled by the intrinsic mobility of each chain and that concentration fluctuations play no role. To test this hypothesis, we have simulated dilute blends with 10 probe chains of type A (or B) in a matrix of 2150 chains of type B (or A). The system size was 60^3, and all chains have a degree of polymerization $N = 10$. Thus, we are simulating a dilute solution of stiff (or flexible) probe chains in a matrix of flexible (or stiff) chains. If intrinsic mobility of chains *alone* control their dynamics in the blend, the dynamics of the dilute probe chains should be identical to the dynamics of a pure melt of those chains and independent of the matrix mobility.

Figure 7a (b) show the diffusion coefficient of a single flexible (or stiff) chain in a matrix of stiff (or flexible) chains as a function of temperature. The corresponding values for the two pure melts are also shown for comparison. Both systems indicate that the dynamics of the probe chains are affected significantly by the matrix. For a flexible probe chain in a stiff matrix (Figure 7a), the probe chain dynamics are identical to those of the matrix at all temperatures. For a single stiff probe chain in a flexible matrix (Figure 7b), the dynamics of the probe chain are slightly slower than those of the matrix chains, particularly at lower temperatures. These results indicate that the dynamics in the system are controlled by the slowest chains. For a single flexible chain in a stiff matrix, the relaxation of the matrix is the rate-determining step. While the flexible chain has a higher intrinsic mobility, it cannot move until the surrounding matrix chains move. The behavior in this limit would thus approach thermorheological simplicity. These observations are in excellent agreement with the diffusion measurements of Kim et al.[24] They have reported that polystyrene (PS, their flexible component) has the same diffusion coefficient as tetramethylpolycarbonate (TMPC, their stiff component) in a TMPC matrix.

In contrast, for a single stiff chain in a flexible matrix, the matrix relaxes faster than the probe chain, and the rate-determining step is the relaxation of the stiff chain itself. Note, however, that the relaxation of the stiff chain is considerably faster than that of a pure melt consisting of stiff chains. Thus, while the stiff chain relaxes slower than the matrix, its dynamics are speeded up by the more mobile matrix. Our findings are similar to literature data, as Kim et al.[24] report that TMPC diffuses a factor of 2 slower than PS in a PS matrix 45 K above the glass transition. Blends in this limit are dynamically heterogeneous, in that each component has a very different Vogel temperature (see Figure 6). This strong difference in mobilities for the single stiff chain and the flexible matrix chains is in qualitative agreement with all blend dynamics models that rely on concentration variations that are limited by chain connectivity.[7,8,10,11,20] The connected nature of polymers does not allow the effective concentration surrounding a stiff monomer to be arbitrarily small. For this reason, the stiff chain monomers must see a very different local environment than the typical flexible chain monomer sees. This creates a large difference in Vogel temperatures of the two components in blends that are rich in the flexible polymer. The apparent minimum in T_0 in Figure 6 is likely not real. We suspect it is a result of the larger uncertainties in the dilute chain dynamics, which naturally arise from poorer statistics on the dilute chains. The poorer statistics, coupled with the smaller temperature range covered, lead to increased uncertainties for the Vogel temperatures of the dilute components.

The situation is quite different for dilute flexible chains in a matrix of stiff chains. While the flexible chain monomers also see a very different local environment than their stiff matrix hosts, there are enough stiff monomers in the local environment to not allow the flexible monomers to move on their own time scale. This asymmetry proves that the dynamics of a polymer in a blend are *not* controlled predominantly by the intrinsic mobility of that chain but are strongly sensitive to its surroundings.

Our observations for dilute low-T_g chains in a matrix of high-T_g chains should be contrasted with the experiments of Ediger, Jones, and co-workers[27] on dilute poly(ethylene oxide) (PEO) in a matrix of poly(methyl methacrylate) (PMMA). These experiments show PEO relaxing 12 orders of magnitude faster than PMMA, a result that is qualitatively expected by the concentration fluctuation models.[9,10,20] Blends of long polymers with weak interactions are predicted to have large fluctuations in local composition that span the entire possible range (from pure PEO to pure PMMA). In the proper temperature range, NMR can detect the motion in regions of pure PEO, and the low T_g of these regions makes segmental dynamics very fast. There are expected to be other regions having the mean blend composition, where PEO segmental dynamics are considerably slower. These dynamics would only be NMR observable at much higher temperatures, owing to the limited dynamic range of NMR.

V. Conclusions

To gain insights into the phenomenon of dynamic heterogeneity in miscible polymer blends, we have simulated a generic polymer blend where the two components have stiffness disparities and no specific interactions. The dynamics of each component in the blend demonstrate that our simulations can capture the essential experimental observations on miscible polymer blends. The two blend components have different temperature dependences to their diffusion coefficients and hence their relaxation times.

The different temperature dependences of diffusion coefficients for the two blend components suggest that they have different Vogel temperatures. The high-T_g component's Vogel temperature agrees well with the Fox equation prediction, indicating that it primarily experiences an environment similar to the mean blend composition. The low-T_g polymer has a lower Vogel temperature than the Fox equation prediction. Polymer blend dynamics models based on concentration fluctuations expect this result as well because the low-T_g monomers can experience environments with very fast dynamics (i.e., environments rich in the low-T_g monomer).

Simulations of dilute blends, consisting of probe chains diffusing in a matrix of dissimilar chains, unequivocally show that the environment surrounding a chain strongly influences its dynamics. This result obviates the notion that intrinsic mobility of chains might control their dynamics, independent of their local environment. Theories for this local environment based on concentration fluctuations and chain connectivity effects are expected to lead to an improved understanding of miscible polymer blend dynamics.

Acknowledgment. Financial support for this work was provided by the National Science Foundation [DMR-9977928]. We thank Mark Ediger for many excellent suggestions.

References and Notes

(1) Colby, R. H. *Polymer* **1989**, *30*, 1275−1278.
(2) Pathak, J. A.; Colby, R. H.; Kamath, S. Y.; Kumar, S. K.; Stadler, R. *Macromolecules* **1998**, *31*, 8988−97.
(3) Zawada, J. A.; Fuller, G. G.; Colby, R. H.; Fetters, L. J.; Roovers, J. *Macromolecules* **1994**, *27*, 6861−6870.
(4) Zawada, J. A.; Fuller, G. G.; Colby, R. H.; Fetters, L. J.; Roovers, J. *Macromolecules* **1994**, *27*, 6851−6860.
(5) Anastasiadis, S. H.; Fytas, G.; Vogt, S.; Gerharz, B.; Fischer, E. W. *Europhys. Lett.* **1993**, *22*, 619−624.
(6) Alegria, A.; Colmenero, J.; Ngai, K. L.; Roland, C. M. *Macromolecules* **1994**, *27*, 4486−4492.
(7) Chung, G. C.; Kornfield, J. A.; Smith, S. D. *Macromolecules* **1994**, *27*, 964−973.
(8) Chung, G. C.; Kornfield, J. A.; Smith, S. D. *Macromolecules* **1994**, *27*, 5729−5741.
(9) Zetsche, A.; Fischer, E. W. *Acta Polym.* **1994**, *45*, 168−175.
(10) Kumar, S. K.; Colby, R. H.; Anastasiadis, S. H.; Fytas, G. *J. Chem. Phys.* **1996**, *105*, 3777−3788.
(11) Lodge, T. P.; McLeish, T. C. B. *Macromolecules* **2000**, *33*, 5278−5284.
(12) Arbe, A.; Alegria, A.; Colmenero, J.; Hoffmann, S.; Willner, L.; Richter, D. *Macromolecules* **1999**, *32*, 7572−7581.
(13) Carmesin, I.; Kremer, K. *Macromolecules* **1988**, *21*, 2819−2823.
(14) Kamath, S. Y.; Colby, R. H.; Kumar, S. K. *Phys. Rev. E* **2003**, *67*, 010801.
(15) Muller, M. *Macromol. Theory Simul.* **1999**, *8*, 343−374.
(16) Muller, M. *Macromolecules* **1995**, *28*, 6556−6564.
(17) Wolfgardt, M.; Baschnagel, J.; Paul, W.; Binder, K. *Phys. Rev. E* **1996**, *54*, 1535−1543.
(18) Kamath, S.; Colby, R. H.; Kumar, S. K.; Baschnagel, J. *J. Chem. Phys.* **2002**, *116*, 865−868.
(19) Wolfgardt, W.; Baschnagel, J.; Binder, K. *J. Phys. II* **1995**, *5*, 1035−1052.
(20) Kamath, S.; Colby, R. H.; Kumar, S. K.; Karatasos, K.; Floudas, G.; Fytas, G.; Roovers, J. E. L. *J. Chem. Phys.* **1999**, *111*, 6121−6128.

(21) Rubinstein, M.; Colby, R. H. *Polymer Physics*; Oxford University Press: New York, 2003.
(22) DeGennes, P. G. *Scaling Concepts in Polymer Physics;* Cornell University Press: Ithaca, NY, 1979.
(23) Saxena, S.; Cizmeciyan, D.; Kornfield, J. A. *Solid State Nucl. Magn. Reson.* **1998**, *12*, 165−181.
(24) Kim, E.; Kramer, E. J.; Osby, J. O. *Macromolecules* **1995**, *28*, 1979−1989.
(25) Salaniwal, S.; Kant, R.; Colby, R. H.; Kumar, S. K. *Macromolecules* **2002**, *35*, 9211−9218.
(26) Pathak, J. A.; Colby, R. H.; Floudas, G.; Jerome, R. *Macromolecules* **1999**, *32*, 2553−2561.
(27) Lutz, T. R.; He, Y.; Ediger, M. D.; Cao, H.; Lin, G.; Jones, A. A. *Macromolecules* **2003**, *36*, 1724−1730.

MA034682X